Comparative characterization of gum rosins for their use as sustainable additives in polymeric matrices

Cristina Pavon[1,], Miguel Aldas[2], Joaquín Hernández-Fernández[3,4], Juan López-Martínez[1]*

C. Pavon, Prof. J. López-Martínez
Instituto de Tecnología de Materiales (ITM), Universitat Politècnica de València (UPV), 03801 Alcoy, Spain.
E-mail: crisppavonv@gmail.com

M. Aldas
Departamento de Ciencia de Alimentos y Biotecnología, Facultad de Ingeniería Química y Agroindustria, Escuela Politécnica Nacional, 170517 Quito, Ecuador.

J. Hernández-Fernández
Centro de investigación e Invención en Ciencias e Ingeniarías, CECOPAT&A, Cartagena 130013, Colombia.
Department of Natural and Exact Sciences, Universidad de la Costa, Calle 58 # 55–66, Barranquilla 080002, Colombia.

There is a growing interest in the use of non-polluting compounds, which come from renewable sources, and which performance in their scope is equivalent to their synthetic similes. In this work, five types of rosins from different sources were studied, verifying the existence of differences that can be inferred in their subsequent use and application as material additives. For the study, rosins were analyzed using gas-mass chromatographic techniques (GC-MS), infrared spectrophotometry (FTIR), differential scanning calorimetry (DSC), thermogravimetric analysis (TGA), and color characterization. The results showed that the samples are composed of either abietic acid or by its structural isomers in contents higher than 80%. FTIR shows that the main difference in the gum rosins is related to the proclivity to absorb environmental moisture and that this technique is not enough to differentiate them. Moreover, the DSC reveals that the gum rosins present enthalpy relaxation effects due to their manufacturing process. The TGA showed that gum rosins are thermally stable until 200 °C, therefore they can be successfully blended with thermoplastic polymers. Finally, the color characterization shows little differences between the samples, being CA the gum rosin with the greatest total color differences.

1. Introduction

In 2020, gum rosin worldwide production volume reached 745 kt. China was the higher producer of gum rosin (320 kt) followed by South America (224 kt), and the rest of Asia (149 kt), while Europe and Central America produced 25 and 22 kt respectively.[1] Gum rosin is a brittle semi-transparent solid mainly composed of diterpenoids, that melts with the increase in temperature.[2],[3] Gum rosin quality and the resin acids content mainly depend on the pine species from which the resin comes.[4],[5] However, the geographical location and the method

of extraction and purification influence its properties and that of its by-products.[2],[6]

According to da Silva et al., (2013) environmental conditions such as water availability, temperature, nutrient access, and plant age will influence the yield that can be obtained from a pine tree.[6]

Chemically, gum rosin contains 90 to 95% of resin acids, whose molecular formula is $C_{19}H_{29}COOH$,[3],[7] and 5 to 10% neutral substances such as alcohols, aldehydes, and hydrocarbons.[5],[8]–[11] The most common resin acids groups in gum rosin are the abietadienes (abietic, levopimaric, palustric and neoabietic) and the pimaradienes (pimaric, isopimaric, and sandaracopimaric acid).[9],[12] On one hand, the abietadienes are presented mainly as carboxylic acids with three fused six-carbon rings and conjugated double bonds. The difference between the abietadiene acids is the position of the conjugated double bonds. However, the four acids are interconvertible passing on heating to an equilibrium mixture in which abietic acid is the major compound and levopimaric acid is scarce.[13] On the other hand, even when the pimaradienes have a similar structure to the abietadienes, one of the double bonds occurs in the alkyl group and it cannot be conjugated with the cyclic double bond. Therefore, the double bonds in pimaradienes are not very reactive.[12],[13]

Gum rosin can be chemically modified into a large number of downstream derivatives.[14] Gum rosin and its derivatives are used in a wide range of applications for instance: cosmetics, adhesives, paper sizing agents, printing inks, surface coatings, insulating materials, and in the food industry.[15],[16] Moreover, new applications are in research in the pharmaceutical industry, for coatings, microencapsulation, and controlled release of substances.[17]–[19] In the polymer area, gum rosin and its derivatives are successfully processed with synthetic thermoplastic polymers and with biopolymers. A gum rosin ester was blended with polyvinyl chloride (PVC) to help stabilize the thermal degradation of PVC.[20] Gum rosin and gum rosin esters were blended with polylactide acid (PLA) and it was determined that they produce a

lubricating effect over PLA polymeric chains.[21] When blended with a Mater-Bi® type biopolymer, gum rosin and its derivatives provide cohesion and plasticization[22],[23]. In a polybutylene adipate co-terephthalate (PBAT) matrix, gum rosin improves the processability and provides plasticization.[24] In blends of PBAT and PLA, gum rosin acts as a size control agent of PBAT domains which allows to improve tensile and impact toughness.[25] Besides, gum rosin is studied in new fields of applications for instance: 3D printing[26] or electrohydrodynamic processes.[18],[27]–[29]

In brief, gum rosin has gained attention as a sustainable additive in polymer matrices, because it allows to enhances the thermal and mechanical behavior of the material and also it lets to reduces production costs.[20],[22],[24] However, from the point of view of materials science, it is necessary to carry out a deeper characterization of gum rosin, to have its most important properties such as composition, functional groups that can interact with other polymers, thermal stability, degradation temperature, glass transition temperature, color. This study is intended to promote the use of gum rosin in polymeric matrices. For this reason, the work analyses and compares five types of commercial gum rosin from different places of origin, to determine their differences and establish their inherent characteristics.

2. Experimental Section

Materials: The study was made on five commercial gum rosins obtained from different origins. (1) gum rosin provided by Aldrich Chemistry (Steinheim, Germany), labeled as CA (softening point of 76 °C and acid number 167); (2) gum rosin from Brazil, provided by Luresa Resinas S.L (Segovia, Spain), labeled as CB (softening point of 76 °C and acid number 167); (3) gum rosin from Spain, provided by Industrial Resinera Valcan S.A. (Cuenca, Spain), labeled as CE; (4) gum rosin from Indonesia, provided by United Resins (Figueira da Foz, Portugal), labeled as CI (softening point of 81 °C and acid number 188);

and, (5) gum rosin from Spain, from the Maritime pine from the Segovia region (labeled as CP).

Methods: Gas chromatography-mass spectrometry (GC-MS) analysis was carried out in an Agilent 5977A mass spectrometer, with a low-resolution quadrupole analyzer, with a gas chromatograph (Agilent 7890B) for capillary columns (split/splitless, pulsed split, and pulsed splitless) and GC-MS interface. Gum rosin samples (3 to 4 mg) were taken into separate test tubes and dissolved with chloroform (0.5 mL). The interface temperature was 280 ºC, in mode: Split 40: 1; with Helium as circulating gas. The initial flow was 1 mL min^{-1} with constant flow. The initial temperature was 60 ºC and was maintained for 5 min. Then, the samples were heated up to 300 °C with a rate of 10 ºC min^{-1} and were maintained at 300 °C for 10 minutes. The injection volume was 3 µl. The apolar capillary column was a 19091S-433U HP-5MS UI (30m - 0.25mm - 0.25mm; apolar), 5% phenylmethyl siloxane, Agilent. Subsequently, the samples have been analyzed using Agilent's "Qualitative" program. The used apolar capillary column was a 19091S-433U HP-5MS UI (30m - 0.25mm - 0.25mm; apolar), 5% phenylmethyl siloxane, Agilent. The sample results were analyzed using Agilent's "Qualitative" program.

Fourier-transform infrared spectroscopy (FTIR) was performed in transmittance mode, in a Perkin Elmer - Spectrum BX (Beaconsfield, UK). Infrared spectra were obtained by using the KBr pellet method. Every sample was assessed in the mid-infrared region from 4000 to 600 cm^{-1}, with 32 scans and 4 cm^{-1} of resolution.

Differential scanning calorimetry (DSC) was conducted in a DSC 821 de Mettler-Toledo Inc. (Schwerzenbach, Switzerland) using samples of 6 mg placed in standard aluminum crucibles with a volume capacity of 40 µl. The thermal cycle consists of a first scan from −40 °C to 170 °C, followed by a cooling cycle from 170 °C to -40 °C, and a second heating scan from −40 °C to 250 °C. The heating and cooling rate in all cycles were 10 °C min^{-1} and the tests were

performed in a nitrogen atmosphere with a flow rate of 30 mL min^{-1}. The first and second heating curves are reported along with the glass transition temperature of each sample.

Thermogravimetric analyses (TGA) were carried out in a thermal analyzer Linseis TGA 1000 (Selb, Germany) using samples with an average weight of 15 mg placed in standard alumina crucibles (70 µl). A dynamic cycle from 30 ºC to 700 ºC at a heating rate of 10 ºC min^{-1} and a nitrogen atmosphere with a flow rate of 30 mL min^{-1} were used. The degradation onset temperature ($T_{5\%}$) was determined at 5% of weight loss, while the maximum degradation temperature (T_{max}) was determined from the maximum at the first derivative of the TGA curve.

The thermal parameters were calculated by the mean value of 3 measurements.

The color of each gum rosin was calculated on a Colorflex-Diff2 458/08 colorimeter from HunterLab (Reston, VA, USA). The test was performed under the CIE L*a*b* color space by finding L*, a*, and b* coefficients. The L* coefficient presents darkness of the color, a* coefficient shows the intensity of green and red colors and b* coefficient shows the intensity of blue and yellow color [30]. The yellow index and the total color differences were also assessed. The mean value of 10 measurements and the standard deviation is reported.

3. Results and discussion

3.1. Gas chromatography-mass spectrometry (GC-MS)

Gas chromatography allowed to separate and identify the molecules in gum rosin, which are presented in Figure 1. Pimaric acid, palustric acid, and abietic acid are structural isomers of each other. Pregn-14-ene (5.beta.), Podocarp-7-en-3-one, 13.beta.-methyl-13-vinyl, and Androst-16-ene-17-carboxylic acid, (5.alpha.) are structural derivatives of the first three acid molecules.

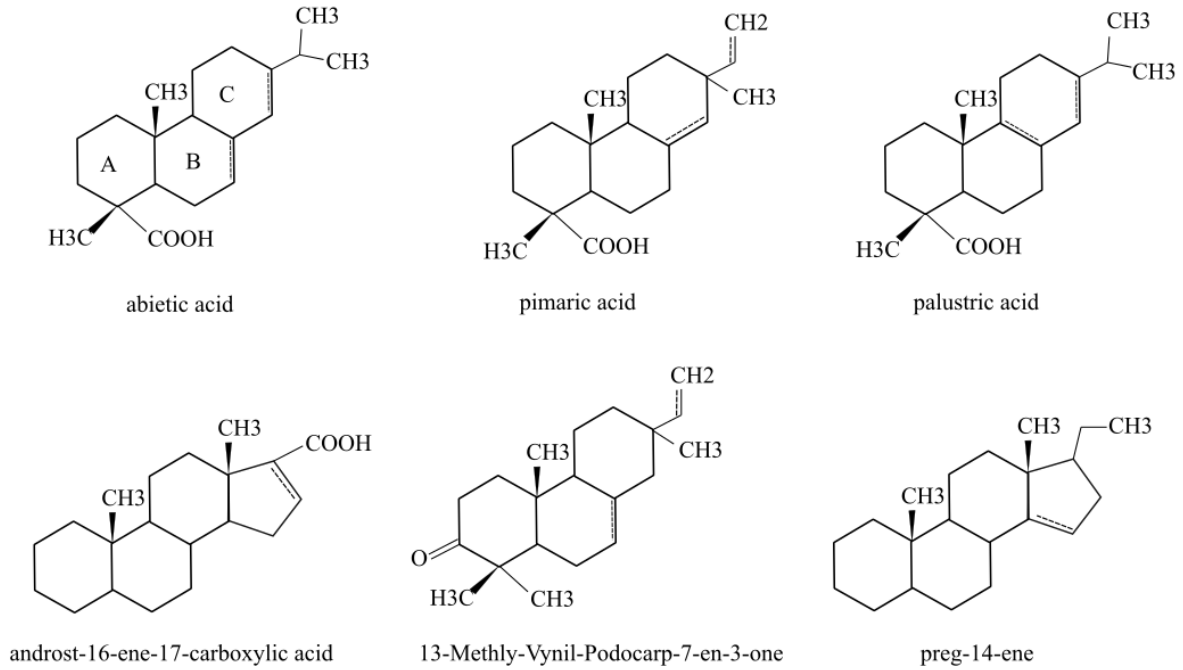

Figure 1. Chemical structure of molecules of interest with greater abundance in the samples

Mass spectrometry was applied due to the presence of structural isomers and to guarantee the correct identification of the molecules. A detailed study of the fragmentation patterns was made to differentiate their structures with high quality. Table 1 shows the used m/z qualifier Ions in this research. Abietic acid presents a fragmentation dominated by m/z = 259 and m/z = 241, which on the one hand produces a fragmentation due to the loss of the carboxyl functional group and, on the other hand, an opening of the A ring by a retro-Diels Alder reaction. m/z 241 ion undergoes successive fragmentation to produce the ions m/z 213, 199, 185, 171, 157, 143, 129 and 128. The greater stability of the most abundant ions in the mass spectrum must be associated with the resonance with the double bond of the B rings. Abietic acid and palustric acidic only differ by the location of their double bonds in C7-C8 y C8-C9.

Table 1. Fragmentation patterns for the compounds of interest

	Pregn-14-ene, (5.beta.)-	Androst-16-ene, 17-carboxylic acid	Pimaric acid	Palustric acid	Podocarp-7-en-3-one, 13.beta.-methyl-13-vinyl-	Abietic acid
	$C_{21}H_{34}$	$C_{27}H_{34}O_3$	$C_{20}H_{30}O_2$	$C_{20}H_{30}O_2$	$C_{20}H_{30}O$	$C_{20}H_{30}O_2$
Qualifier Ion m/z	79	91	93.1	91.1	67	91.1
	91	107	105	105.1	79	105.1
	107	121	119.1	121.1	91	121.1
	123	135	121.1	131.1	105	131.1
	133	145	131	133.1	119	135.1
	147	190	133.1	185.1	131	213.2
	161	241	185.1	239.2	145	241.2
	187	257	241.2	241.2	159	259.2
	201	287	287.2	287.2	171	287.2
	243	302	302.2	302.2	187	302.2
	257				201	
	271				215	
					229	
					243	
					257	
					271	

The structure of pimaric acid, presents the absence of a double bond in ring B, as observed in Figure 1. This allows a different fragmentation to occur, leading to the formation of fragments in m/z 121, 120, 105 y 91. The possible pathways leading to the fragments involve the formation of intermediate ion in m/z = 239, which is formed by a Diels Alder reaction and this fragment can only be formed by the absence of the double bond in ring B and the presence of a double bond in C8 in-ring C. m/z 121 and 120 fragments are specific for the C8 = C14 double bond, therefore, they provide valuable structural information. Degradation of m/z 257 ion generates characteristic fragments as m/z 242, 227, 215, 201, and 187 and others related that present m/z of 173, 161, 147, and 133. Palustric acid has two double bonds in the C ring, as shown in Figure 1. The spectra of palustric acid show intense peaks corresponding to the fragment's m/z 241. The formation of the fragments most likely involves the

mechanism of rupture of ring A and the subsequent generation of ions, without fragmentation of rings B and C.

Table 2 lists the most significant components of each of the samples of interest. Pimaric acid, palustric acid and abietic acid were the compounds with the highest abundance. Piramic acid and abietic acid, showed similar retention time, Tr = 26.0 min, while palustric acid showed a Tr = 26.67 min. Figure 2 shows the percentage of the molecules of interest with the highest abundance each rosin gum rosin. CA, CE, CI, and CP contain mainly abietane-type acids, while CB is constituted by a mixture of abietane and pimarane-type acids. CE and CA contain 96% abietic acid as the major component but differ in the type and content of minority compounds. CI contains 98% palustric acid. Abietic acid was also the major component in CP, with a concentration of 87%. CB is constituted by 5% of palustric acid and 82% of pimaric acid. These results suggest that CA, CE, CP, and CI can be more easily chemical modified as they present a conjugated double bond in their structure.[31] However, this reactiveness made them susceptible to air oxidation turning them into allergenic compounds.[16]

Table 2. Compounds of greatest significance in the characterization retention time and area

Tr (min)	Empirical formula	Compund namename	Units	CB	CI	CE	CA	CP
6,693	$C_{10}H_{16}$	Tricyclo[2.2.1.0(2,6)]heptane, 1,3,3-trimethyl-	% area	0	0	0	0	11.28
15,356	$C_{15}H_{24}$	Naphthalene, 1,2,3,5,6,7,8,8a-octahydro-1,8a-dimethyl-7-(1-methylethenyl)-, [1R-(1.alpha.,7.beta.,8a.alpha.)]-	% area	0	0	0.75	0	0
23,639	$C_{21}H_{34}$	Pregn-14-ene, (5.beta.)-	% area	1.02	0	0.5	0.48	0
24,121	$C_{20}H_{30}O$	Podocarp-7-en-3-one, 13.beta.-methyl-13-vinyl-	% area	2.07	1.12	0.59	0	0
24,517	$C_{31}H_{33}NO_2$	Benzoic acid, 4-(4-pentylcyclohexyl)-, 4'-cyano[1,1'-biphenyl]-4-yl ester	% area	0	0	0	0,52	0
24,852	$C_{20}H_{30}O$	4,14-Retro-retinol	% area	1.26	0	0	0	0
25,041	$C_{22}H_{18}O_5$	Phthalic acid, 4-methoxyphenyl 3-methylphenyl ester	% area	0	0.66	0.56	0.39	0
25,05	$C_{27}H_{34}O_3$	Androst-16-ene-17-carboxylic acid, (5.alpha.)	% area	5.37	0	0	0	0
26,005	$C_{20}H_{30}O_2$	Pimaric acid	% area	81.7	0	0	0	0
26,022	$C_{20}H_{30}O_2$	Abietic acid	% area	0	0	95.77	96.47	87.29
26,358	$C_{16}H_{14}O_3$	Isoparvifuran	% area	0	0	0	0	0
26,667	$C_{20}H_{30}O_2$	Palustric acid	% area	4.97	97.54	0	0	0

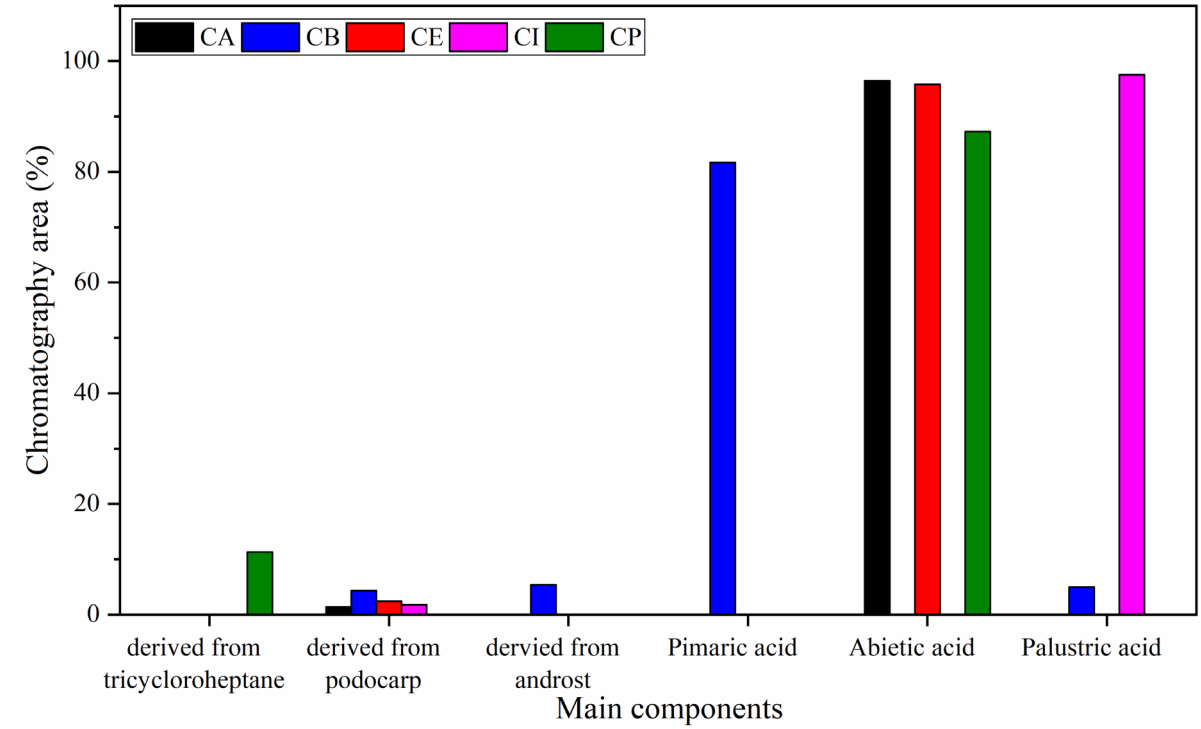

Figure 2. Molecules of interest with greater abundance in the samples of interest

3.2. Fourier Transform Infrared Spectroscopy (FTIR)

The infrared spectra of the five studied gum rosins are presented in Figure 3. For analysis purposes, the spectra can be divided into four zones as follows: (1) the OH region located between 3700 – 3200 cm^{-1}; (2) the carbonyl region found between 1800 – 1550 cm^{-1}; (3) the CH region located between 3200 – 2400 cm^{-1} and, (4) the fingerprint region located between 1550 – 600 cm^{-1}.[32]–[34]

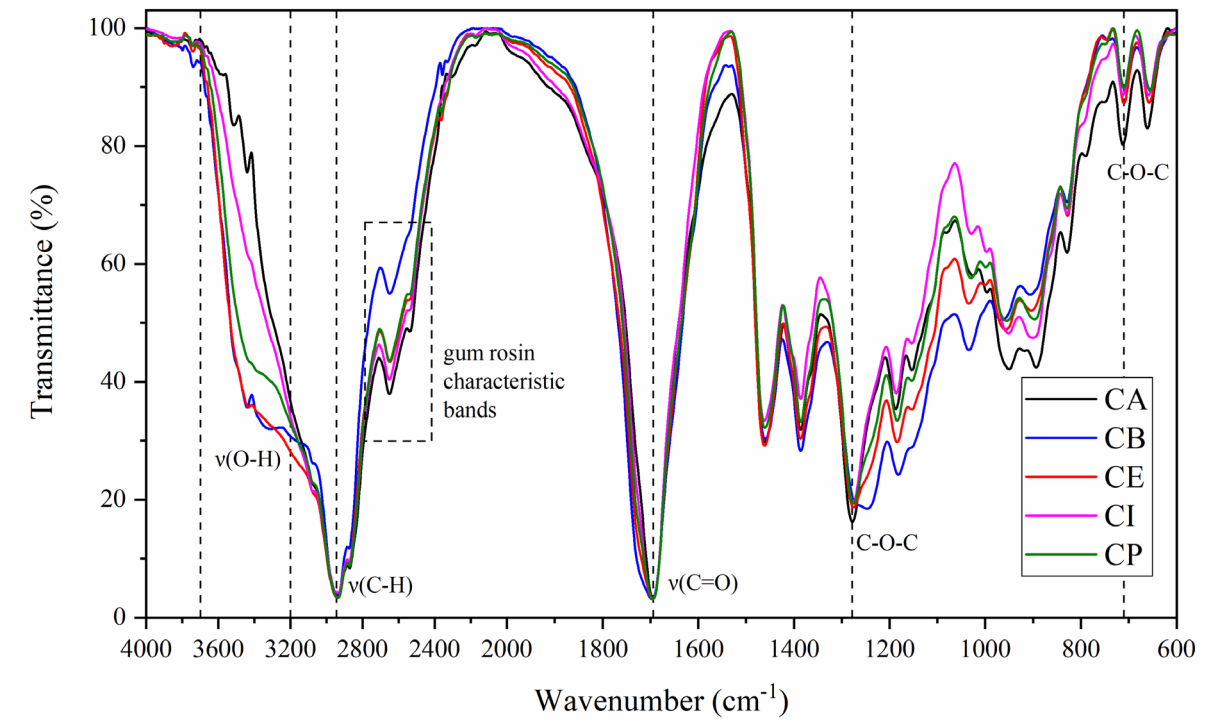

Figure 3. Fourier-transform infrared spectroscopy (FTIR) spectra of gum rosins from different origins

The band corresponding to a stretching bond ν(O-H) of the functional group -COOH is presented as a shoulder at 3336, 3376, and 3378 cm^{-1} in CB, CP, and CE respectively. In CI and CA, this peak is less notorious and is found as an inflection at 3402 cm^{-1} and 3332 cm^{-1} respectively.[33] This indicates that CB, CP, and CE contain moisture from the environmental humidity.[35] In all gum rosins, a peak with a maximum at 2944 cm^{-1} and a small append peak at 2872 cm^{-1} indicates the strong stretching vibration modes C–H of the methyl and methylene group due to the hydrocarbon structures with three rings typical of diterpenes.[35] Moreover, the characteristic band to identify gum rosin was found as a broad double structured band with peaks at 2652 and 2536 cm^{-1}. This band corresponds to the overtone stretching of the carboxyl group.[35] The characteristic band of carboxylic acid bonding ν(C=O) is observed at 1694 cm^{-1}.[9],[33] Finally, in the fingerprint region, between 1500 and 600 cm^{-1}, the absorption bands found between 1200 cm^{-1} and 800 cm^{-1} are characteristic of diterpenic resins,[32] while specific bands of gum rosin are at 1278 (C-O-C) and 712 cm^{-1}.[32] Between 1500 and 1000 cm^{-1}, the presence of several bands related to binding stretches ν(C-C) of the hydrocarbon

chain of gum rosin,[33] and bonds type ν(C=C) and ν(C-O) are seen with different intensity in each gum rosin.[36]

The mention peeks are consistent with the presence of resinous acids[33] and were previously reported by other researchers.[32],[33],[35],[36] As seen in Figure 3, the five spectra resemble each other as the chemical composition of gum rosins are close to each other. However, the main differences seem to be located in the fingerprint region which can be attributed to the gum rosin pine source and predominant resin acid,[36] and in the predisposition to absorb moisture (stretching bond ν(O-H) of the samples.

3.3. Differential Scanning Calorimetry (DSC)

Differential scanning calorimetry (DSC) was used to assess the thermal properties of the samples.[37]–[39] The first and second DSC heating curves are shown in Figure 4. The first heating curve (Figure 4-a) leads to determined that the samples have different thermal histories related to the processing or storage conditions,[40],[41] seen on DSC as an endothermic peak in the glass transition region (from 25 °C to 70 °C). This endothermic peak is known as the enthalpy relaxation effect (marked between red dashes).[40],[42] The enthalpy relaxation effect occurs when the material is heated through T_g and took place to relieve the excess enthalpy associated with molecular stress.[42],[43] This phenomenon indicates that gum rosins have been heated and cooled quickly in their processing. Therefore, the molecules were "frozen" into high-energy conformations.[43] Fast heating and cooling are performed to achieve gum rosin with a high content of only one abietadiene or pimaradiene compound.[13]

It is seen that the relaxation effect in CA, CE, and CI is presented in one or two steps. In the other samples, various peaks of enthalpy excess are detected. The location and magnitude of these peaks are a function of the thermal treatment and polymer structure.[42] CA present the highest excess of enthalpy in this region with a value of 6.30 J g^{-1}. Additionally, a small endothermic peak appears between 100 and 125 °C in the first heating curve of all the

samples (blue arrows). This peak might be caused by the presence of residual volatiles, and is sharper in CA, CB, and CP, than in CE and CI.[41]

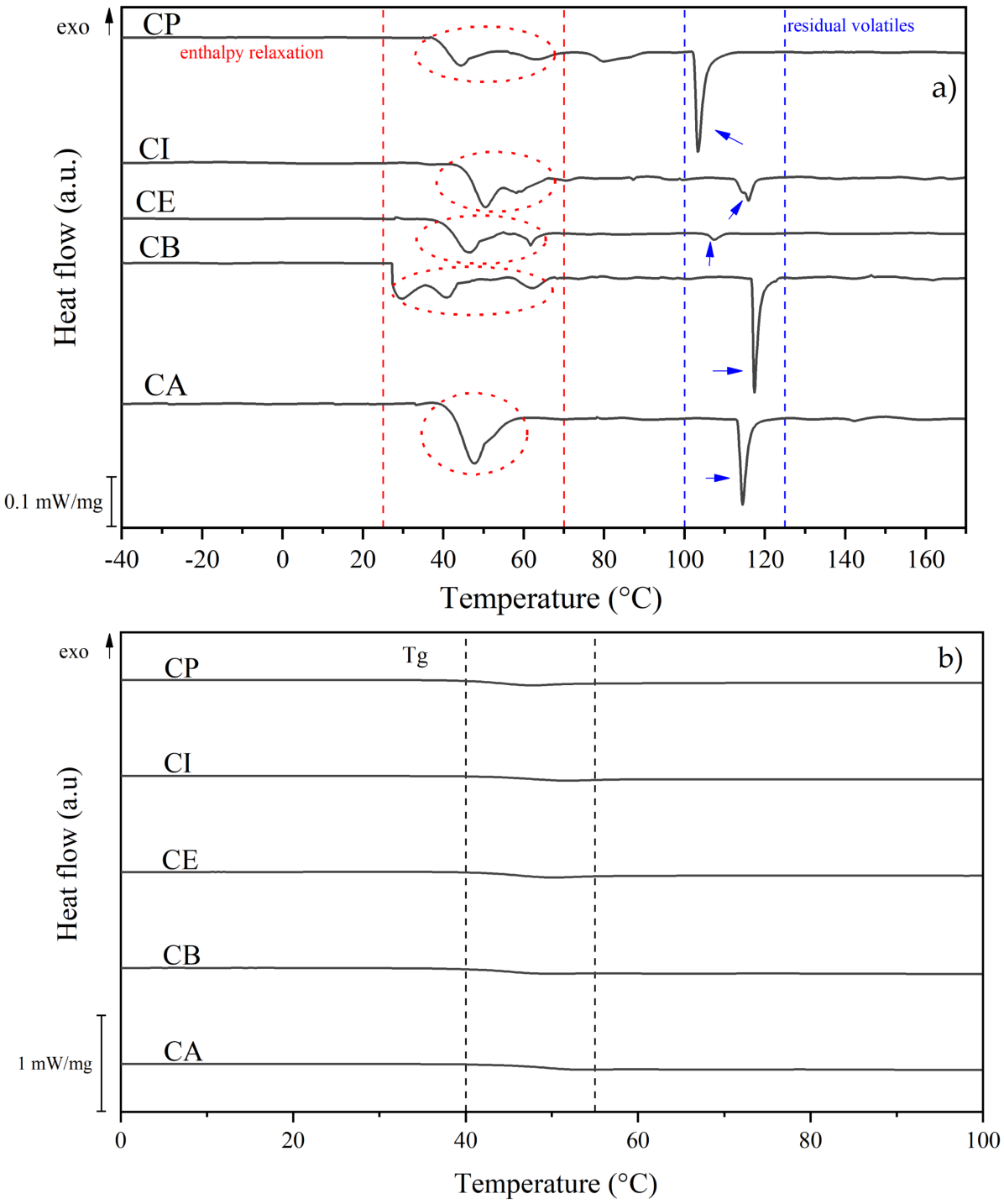

Figure 4. DSC first (a) and second heating (b) curves of five different gum rosins

In the second heating curve (Figure 4-b), an inflection attributed to gum rosin glass transition (T_g) is observed between 40 °C to 50 °C for all the samples. T_g values are presented in Table

3. T_g values agreed with the range reported by Cabaret et al. (2018) for industrial gum rosin [9]. The value of T_g in CA and CI presents no statistical differences ($p < 0.05$) among them, as well as T_g of CB, CE and CP.

Table 3. Thermal transitions of the different gum rosins during the DSC first and second heating, and thermal stability parameters for studied gum rosins

	DSC			TGA	
	First heating		Second heating		
Sample	ΔH_1 (J g $^{-1}$)	ΔH_{2m} (J g $^{-1}$)	T_g (°C)	$T_{5\%}$ (ºC)	T_{max} (ºC)
CA	-6.30	-1.73	48.4 ± 0.8^{a}	230 ± 2^{a,b}	315 ± 1^{a}
CB	-4.33	-1.59	44.2 ± 0.7^{b}	223 ± 1^{a}	322 ± 2^{b}
CE	-5.29	-0.42	45.4 ± 0.6^{b}	200 ± 10^{c}	311 ± 1^{c}
CI	-4.29	-0.14	47.4 ± 0.7^{a}	232 ± 1^{b}	315 ± 1^{a}
CP	-4.82	-0.57	43.8 ± 0.4^{b}	236 ± 4^{b}	309 ± 1^{c}

$^{a-d}$ Different letters within the same property show statistically significant differences between formulations ($p < 0.05$)

3.4. Thermogravimetric analyses (TGA)

Thermogravimetric curves (TGA) and their derivative (DTG) of the five studied gum rosins are shown in Figure 5. In Figure 5-a four main weight-loss stages are observed in CA, CE, CI, and CP and three stages in CB. In CB, CE, and CA the first weight-loss stage takes place at 105 °C and is attributed to absorbed moisture.[35],[44] In the case of CB and CE, the presence of moisture is in accordance with the FTIR results that show large and wide OH peaks in their spectra. CB and CE lose 3 % of their mass due to evaporation, while CA loss 1.8 % of the initial mass. Furthermore, as CI and CP do not present a significant amount of absorbed water, as seen in the infrared spectra Figure 3, they do not show a weight loss in this stage. Between 200 °C up to 350 °C, the decomposition of the organic components takes place, with a mass loss of 70 % in all the samples.[33] This stage corresponds with the maximum decomposition temperature, which is verified with the minimum of the DTG curves (Figure 5-b). In this range, the evaporation of the sesquiterpenes also takes place (which have a boiling point of 272 °C [35]) present in the resins.

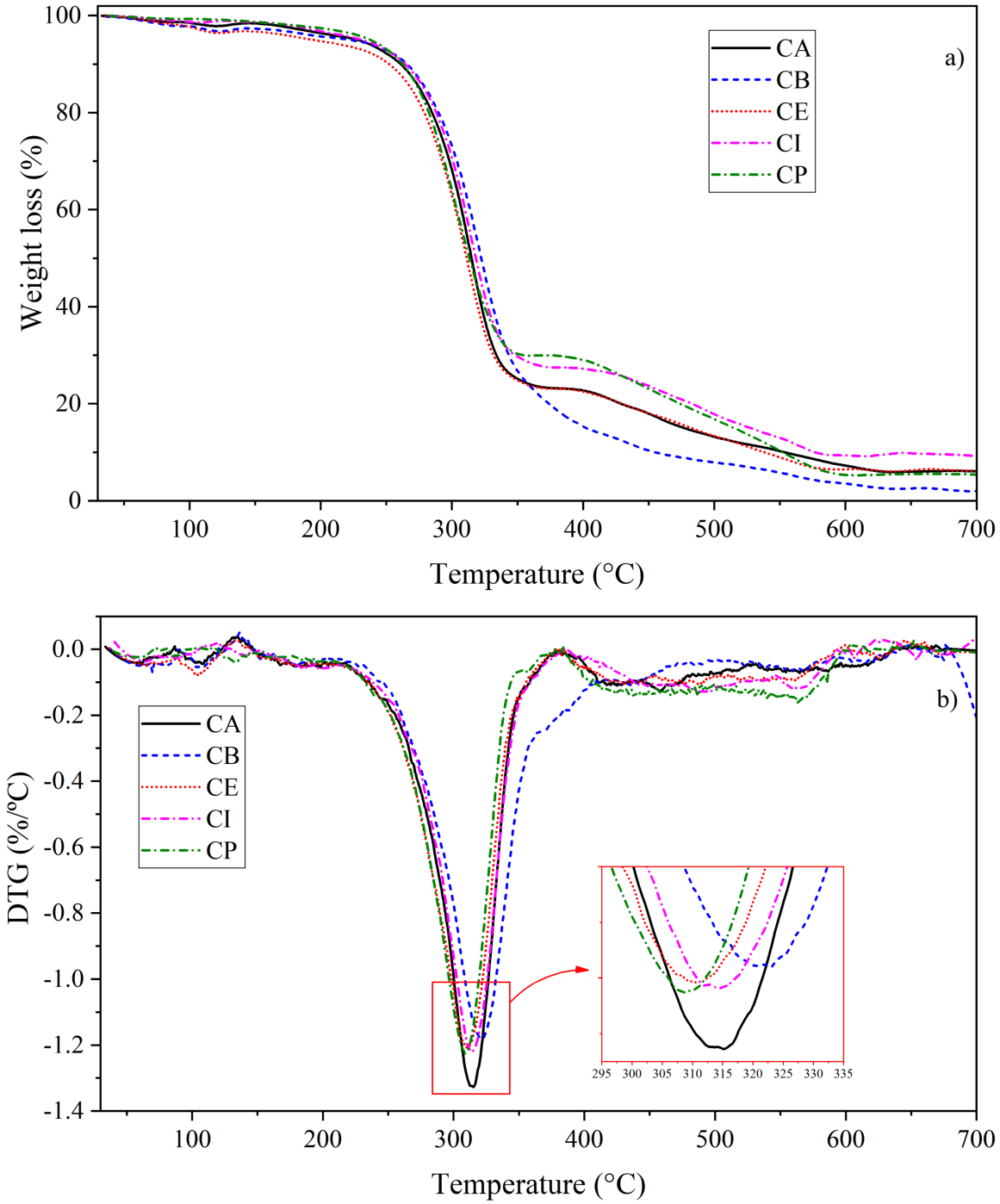

Figure 5. (a) TGA curves and (b) DTG curves with an expanded area for temperatures between 295 ◦C and 335 ◦C for the five studied gum rosins

For CA, CE, CI, and CP, the third weight loss, detected up to 570 °C is attributed to a phase transition, evaporation of resin compounds, and pre-carbon formation.[35],[45] In this step, 90% of mass loss is reached in all studied samples. The last stage of decomposition (in temperatures above 570 °C) is related to the degradation of the structure.[45] At the end of the test, the mass of CA, CE, and CP was 6%, CB keeps 2 %, and CI a 10 % with respect to the

initial mass. TGA results of the gum rosins showed good thermal stability. The decomposition of the organic material starts at 150 °C and the total decomposition of the material was found at approximately 600 °C, for all the studied samples. The obtained curves showed in Figure 5 are in good agreement with the literature.[9],[35],[44] As well, the temperatures of maximum degradation rate (T_{max}) obtained from Figure 5-b are reported in Table 3. It is seen that CA and CI present no statistical differences ($p > 0.05$) in T_{max} as well as CE and CP. Whereas, the T_{max} of CB is 7 ° C higher than CA and CI, and 10 °C higher than CE and CP. Regarding. The onset degradation temperature ($T_{5\%}$) of CA, CI, and CP have the highest values among all the samples, above 230 °C, while CE has the lowest, at 200 °C. This result suggests that gum rosin can be used as an additive in materials which processing temperatures are lower than 200 °C, with no significant effect on its thermal behaviour.

3.5. Colour measurements

CIEL*a*b* color coordinates for the five gum rosins studied are shown in Figure 7. A photograph of the five different gum rosin showing their respective coloration is presented in Figure 6. The lightness coordinate L* shows that the samples are medium-lighted and that CA is the one with the highest luminosity. The a* coordinate of all the samples has values near 0, which means that red and green hue are not dominant in those samples, except for CI which value (2.2) points to a reddish hue (see Figure 6-d). Also, it was determined that there are no statistical differences in the a* coordinate between CA and CP and between CP and CE. The b* coordinate results allowed to establish that all the samples have a yellowness hue because the yellow coloration is inherent of gum rosin. Moreover, it was determined, that there are no statistical differences between CB and CI, and between CE and CP in the b* coordinate. CA is the sample with the highest b* value while CE and CP the ones with the lowest b* value. The yellowish coloration of gum rosin will directly affect the color of the final material when used as an additive as seen by Aldas et al. (2021)[46] and Pavon et al. (2020).[26]

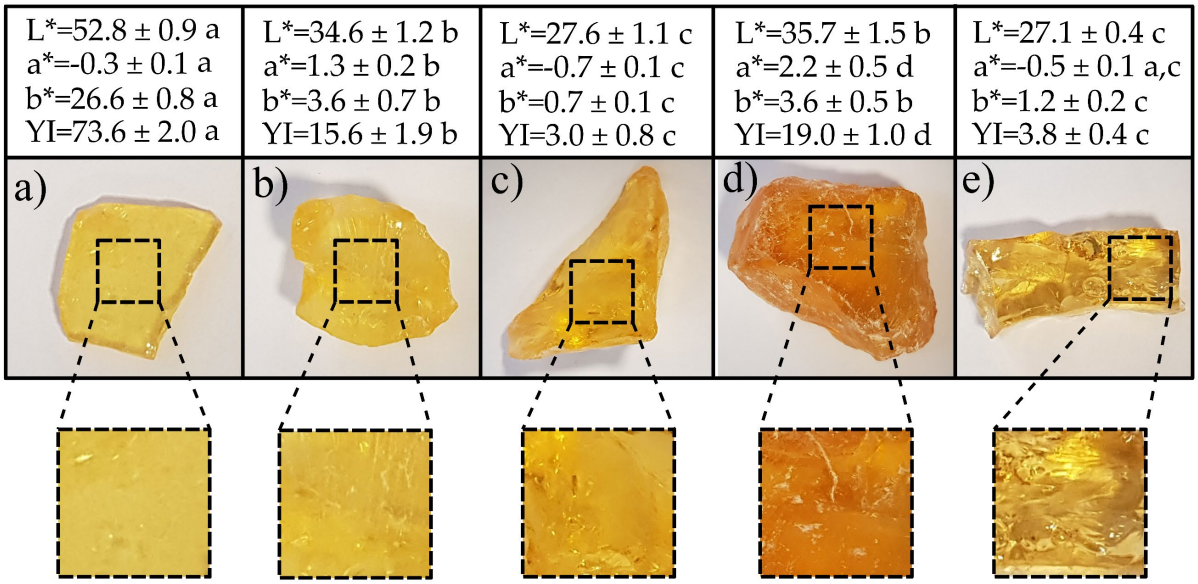

[a-d] Different letters within the same property show statistically significant differences between formulations ($p < 0.05$)

Figure 6. Gum rosin samples color of a) CA, b) CB, c) CE, d) CI and e) CP

All the samples present a yellowness index (YI) due to the inherent coloration of gum rosin, therefore, these values are in accordance with the b* parameter. The YI shows that CA is the sample with the high yellow coloration. CB and CI have no statistical differences in the YI. The YI in CE and CP have the lowest YI and they present no statistical differences in the YI values among them.

4. Conclusions

Five gum rosins from different places were characterized. Each gum rosin has its characteristics which must be considered when using them as additives for polymeric materials. Gas chromatography-mass spectrometry (GC-MS) determined that there is a variation in the acid type and content of each gum rosin. CA, CB, and CP have high contents of abietic acid, CB presents a mixture between pimaric acid and palustric acid, while CI is composed mainly of palustric acid. The respective composition of each gum rosin is useful for the intended application. Abietadiene acids are preferable if gum rosin modification will be performed, pimaradienes are desirable if the application will be in direct contact with the skin. FTIR spectra of the five gum rosins showed that the characteristic groups of unmodified gum

rosin and that CB, CE, and CP have a predisposition to absorb moisture. DSC shows that the processing of the material has a direct effect on the thermal characteristics of gum rosins. TGA proves that the five studied gum rosins have good thermal stability. Therefore, gum rosin can be used as an additive in thermoplastic polymers which processing temperatures do not exceed 200 °C (in the case of CE) or 230 °C (in the case of CA, CI, CB and CP). The color measurements let to prove there is a variation in the color properties of each gum rosin. Moreover, the inherent yellowish coloration of gum rosins will directly affect the color of the final material when used as an additive. As a natural additive gum rosin has a great potential to be used as a natural additive in biodegradable polymers, where it can guarantee the eco-friendly nature of the products.

Acknowledgments

This research was funded by the Spanish Ministry of Science and Innovation project: PID2020-116496RB-C22. Cristina Pavon thanks Santiago Grisolía fellowship (GRISOLIAP/2019/113) from Generalitat Valenciana. The authors thank Funding for open access charge: CRUE-Universitat Politècnica de València.

Received: ((will be filled in by the editorial staff))
Revised: ((will be filled in by the editorial staff))
Published online: ((will be filled in by the editorial staff))

References

[1] Harima Chemicals Group Inc. Rosin Production and Rosin Market. https://www.harima.co.jp/en/pine_chemicals/rosin3.html (accessed August 17, 2021).

[2] Yadav, B. K.,Gidwani, B.,and Vyas, A. *J. Bioact. Compat. Polym.* **2016**, *31*, 111.

[3] Mitchell, G.,Gaspar, F.,Mateus, A.,Mahendra, V.,and Sousa, D. *Advanced Materials from Forests*; **2018**.

[4] Gallo Corredor, J. .,and Sarria Villa, R. . *J. Cienc. e Ing.* **2014**, *6*, 65.

[5] Karlberg, A.-T. In *Handbook of Occupational Dermatology*; Springer Berlin Heidelberg: Berlin, Heidelberg, **2000**; pp 509.

[6] da Silva, K.,de Lima, J.,and Fett-Neto, A. In *Natural Products: Phytochemistry, Botany*

and Metabolism of Alkaloids, Phenolics and Terpenes; **2013**; pp 1.

[7] Silvestre, A. J. D.,and Gandini, A. In *Monomers, Polymers and Composites from Renewable resources*; Elsevier Ltd., **2008**; pp 67.

[8] Wiyono, B.,Tachibana, S.,and Tinambunan, D. *Indones. J. For. Res.* **2016**, *3*, 7.

[9] Cabaret, T.,Boulicaud, B.,Chatet, E.,and Charrier, B. *Eur. J. Wood Wood Prod.* **2018**, *76*, 1453.

[10] Mason Joye, N. J.,and Lawrence, R. V. *J. Chem. Eng. Data* **1967**, *12*, 279.

[11] Wiyono, B.,Tachibana, S.,and Tinambunan, D. *Indones. J. For. Res.* **2006**, *3*, 7.

[12] Valto, P.,Knuutinen, J.,and Alén, R. *BioResources* **2012**, *7*, 6041.

[13] Mills, J. S.,and White, R. *Stud. Conserv.* **1977**, *22*, 12.

[14] Maiti, S.,Ray, S. S.,and Kundu, A. K. *Prog. Polym. Sci.* **1989**, *14*, 297.

[15] Wilbon, P. A.,Chu, F.,and Tang, C. *Macromol. Rapid Commun.* **2013**, *34*, 8.

[16] Karlberg, A.-T. In *Kanerva's Occupational Dermatology,*; **2012**; Vol. 1–3, pp 467.

[17] Pratapwar, A. .,and Sakarkar, D. . *J. Qual. Assur. Pharma Anal.* **2015**, *1*, 100.

[18] Baek, W. Il,Nirmala, R.,Barakat, N. A. M.,El-Newehy, M. H.,Al-Deyab, S. S.,and Kim, H. Y. *Appl. Surf. Sci.* **2011**, *258*, 1385.

[19] Kumar, S.,and Gupta, S. K. *Polim. Med.* **2013**, *43*, 45.

[20] Arrieta, M. P.,Samper, M. D.,Jiménez-López, M.,Aldas, M.,and López, J. *Ind. Crops Prod.* **2017**, *99*, 196.

[21] de la Rosa-Ramirez, H.,Aldas, M.,Ferri, J. M.,Samper, M. D.,and Lopez-Martinez, J. *J. Appl. Polym. Sci.* **2020**, *137*, 49346.

[22] Aldas, M.,Pavon, C.,López-Martínez, J.,and Arrieta, M. P. *Appl. Sci.* **2020**, *10*, 2561.

[23] Aldas, M.,Ferri, J. M.,Lopez-Martinez, J.,Samper, M. D.,and Arrieta, M. P. *J. Appl. Polym. Sci.* **2020**, *137*, 48236.

[24] Pavon, C.,Aldas, M.,de la Rosa-Ramírez, H.,López-Martínez, J.,and Arrieta, M. P. *Polymers (Basel).* **2020**, *12*, 2891.

[25] Aldas, M.,Ferri, J. M.,Motoc, D. L.,Peponi, L.,Arrieta, M. P.,and López-Martínez, J. *Polymers (Basel).* **2021**, *13*, 1913.

[26] Pavon, C.,Aldas, M.,López-Martínez, J.,and Ferrándiz, S. *Polymers (Basel).* **2020**, *12*, 334.

[27] Nirmala, R.,Woo-il, B.,Navamathavan, R.,Kim, H. Y.,and Park, S.-J. *J. Nanosci. Nanotechnol.* **2015**, *15*, 4653.

[28] Pavon, C.,Aldas, M.,De La Rosa-Ramírez, H.,Samper, M. D.,Arrieta, M. P.,and López-Martínez, J. *Polym. Adv. Technol.* **2021**, pat. 5397.

[29] Pavon, C.,Aldas, M.,Rayón, E.,Arrieta, M. P.,and López-Martínez, J. *Environ. Technol. Innov.* **2021**, *24*, 101812.

[30] Weatherall, I. L.,and Coombs, B. D. *Skin Color Measurements in Terms of CIELAB Color Space Values*; **1992**; Vol. 99.

[31] El-Ghazawy, R. A.,El-Saeed, A. M.,Al-Shafey, H. I.,Abdul-Raheim, A. R. M.,and El-Sockary, M. A. *Eur. Polym. J.* **2015**, *69*, 403.

[32] Azémard, C.,Vieillescazes, C.,and Ménager, M. *Microchem. J.* **2014**, *112*, 137.

[33] Correa, J. de S.,dos Santos, R. R.,and Anaissi, F. J. *Orbital* **2018**, *10*, 200.

[34] Kizil, R.,Irudayaraj, J.,and Seetharaman, K. *J. Agric. Food Chem.* **2002**, *50*, 3912.

[35] Favvas, E. P.,Kouvelos, E. P.,Papageorgiou, S. K.,Tsanaktsidis, C. G.,and Mitropoulos, A. C. *Appl. Phys. A Mater. Sci. Process.* **2015**, *119*, 735.

[36] Sifontes, Á. B.,Gutierrez, B.,Mónaco, A.,Yanez, A.,Díaz, Y.,Méndez, F. J.,Llovera, L.,Cañizales, E.,and Brito, J. L. *Biotechnol. Reports* **2014**, *4*, 21.

[37] Gill, P.,Moghadam, T. T.,and Ranjbar, B. *J. Biomol. Tech.* **2010**, *21*, 167.

[38] Chiu, M. H.,Berezowski, N. S.,and Prenner, E. J. In *Drug-Biomembrane Interaction Studies*; Elsevier, **2013**; pp 237.

[39] Kodre, K.,Attarde, S.,Yendhe, P.,Patil, R.,and Barge, V. *Res. Rev. J. Pharm. Anal.* **2014**, *3*, 11.

[40] Groenewoun, W. M. In *Characterisation of Polymers by Thermal Analysis*; Elsevier, **2001**; pp 10.

[41] Hohne, G. W. H.,Hemminger, W.,and Flammersheim, H.-J. *Differential Scanning Calorimetry*; **2019**; Vol. 53.

[42] Runt, J.,and Huang, J. In *Handbook of Thermal Analysis and Calorimetry*; **2002**; Vol. 3, pp 273.

[43] Parker, M. J. In *Comprehensive Composite Materials*; **2000**; pp 183.

[44] Lazzarotto, M.,Zavattieri Ruiz, H.,da Silveira Lazzarotto, R. S.,Schnitzler, E.,Teixeira,Teixeirade Moraes, M. L.,Cambuim, J.,dos Santos, W.,and de Aguiar, A. V. In *IX Congresso Brasileiro de Análise Térmica e Calorimetria 09 a 12 de novembro de 2014 – Serra Negra – SP - Brasil Use*; **2014**; pp 1.

[45] Tsanaktsidis, C. G.,Favvas, E. P.,Scaltsoyiannes, A. A.,Christidis, S. G.,Katsidi, E. X.,and Scaltsoyiannes, A. V. *Fuel Process. Technol.* **2013**, *114*, 135.

[46] Aldas, M.,Pavon, C.,Ferri, J. M.,Arrieta, M. P.,and López-Martínez, J. *Polymers (Basel).* **2021**, *13*, 1506.